

Attaching Metal-Capped sp Carbon Chains to Metal Clusters: Synthesis, Structure, and Reactivity of Rhenium/Triosmium Complexes of Formula $[(\eta^5\text{-C}_5\text{Me}_5)\text{Re}(\text{NO})(\text{PPh}_3)(\text{CC})_n\text{Os}_3(\text{CO})_y(\text{X})_z]^m+$, Including Carbon Geometries More Distorted than Planar Tetracoordinate

Stephen B. Falloon, Slawomir Szafert, Atta M. Arif, and J. A. Gladysz*

Abstract: Reaction of $[(\eta^5\text{-C}_5\text{Me}_5)\text{Re}(\text{NO})(\text{PPh}_3)(\text{C}\equiv\text{CH})]$ (**1**) and $[\text{Os}_3(\text{CO})_{10}(\text{NCCCH}_3)_2]$ (CH_2Cl_2 , room temperature) gives the ReC_2Os_3 complex $[(\eta^5\text{-C}_5\text{Me}_5)\text{Re}(\text{NO})(\text{PPh}_3)(\text{CC})\text{Os}_3(\text{CO})_{10}(\text{H})]$ (**2**, 78%). The crystal structure shows that the hydride and ReCC terminus bridge the same two osmium atoms symmetrically. The $\text{Re}-\text{C}$ and $\text{ReC}-\text{C}$ bond lengths, and IR and NMR properties, indicate contributions by both $\text{ReC}\equiv\text{C}(\text{Os}_3)$ and $^+\text{Re}=\text{C}=\text{C}(\text{Os}_3)^-$ resonance forms. Analogous ReC_4Os_3 (**4**, 83%) and ReC_6Os_3 (**6**, 61%) complexes are prepared similarly, and are increasingly less stable

in solution and the solid state. Cyclic voltammograms of **2**, **4**, and **6** show partially reversible oxidations. Complex **4** decarbonylates in refluxing hexane to give $[(\eta^5\text{-C}_5\text{Me}_5)\text{Re}(\text{NO})(\text{PPh}_3)(\text{CCC}-\text{C})\text{Os}_3(\text{CO})_9(\text{H})]$ (**7**, 57%), in which the ReCCCC terminus binds to three osmium atoms, and the adjacent carbon (and hydride) to two. Reaction of **2** and $\text{HBF}_4 \cdot \text{Et}_2\text{O}$ gives $[(\eta^5\text{-C}_5\text{Me}_5)\text{Re}(\text{NO})(\text{PPh}_3)(\text{CC})\text{Os}_3(\text{CO})_{10}(\text{H})_2]^+ \cdot \text{BF}_4^-$ (**8**⁺ BF_4^- , 69%). The crystal structure of the

SbF_6^- salt shows an ReC_2Os_3 unit very similar to that of **2**, but with the hydrides bridging different osmium–osmium bonds. The C_3OME complex $[(\eta^5\text{-C}_5\text{Me}_5)\text{Re}(\text{NO})(\text{PPh}_3)(\text{C}\equiv\text{CC}(\text{OMe})=)\text{Os}_3(\text{CO})_{11}]$ (**9**) decarbonylates in refluxing heptane to give $[(\eta^5\text{-C}_5\text{Me}_5)\text{Re}(\text{NO})(\text{PPh}_3)(\text{CCC})\text{Os}_3(\text{CO})_9(\text{OMe})]$ (**10**, 63%), in which the ReCCC terminus binds to three osmium atoms, and the center carbon binds to the osmium that is not methoxide-bridged. The crystal structure shows the ReCCC carbon to be highly distorted, binding to four atoms that fall on one side of a plane through the carbon.

Keywords: carbon chains • clusters • cumulenes • osmium • rhenium

Introduction

Complexes in which sp carbon chains span transition metal endgroups are attracting increasing attention.^[1–4] These wire-like, unsaturated linear assemblies offer aesthetic appeal, a variety of interesting fundamental properties, and intriguing possibilities for molecular-level devices.^[5] Most such compounds feature monometallic termini. However, polymetallic termini might confer special attributes, which could include enhanced electronic coupling or communication between the endgroups, altered hyperpolarizabilities, and access to larger numbers of redox states.

We were attracted by the architectural versatility of trimetallic clusters, which should allow many modes of chain attachment. When only the terminal carbon coordinates, three types of junctions are possible, as depicted in Figure 1: **A**, a μ_1 link to one metal; **B**, an edge-bridging μ_2 link to two

metals; and **C**, a face-bridging μ_3 link to three metals. In all cases, the terminal carbon may serve as a one-, two-, or three-electron donor, depending upon the electronic requirements of the cluster. It should also be noted that in **B** and **C** the terminal carbon may be sp²- or sp³-hybridized instead of being sp-hybridized.

There is extensive literature on metal cluster carbide complexes,^[6] some of which provides models for surface-bound intermediates in commodity-chemical processes that are heterogeneously catalyzed. However, only a few contain sp carbon segments that span otherwise unconnected polymetallic termini.^[3d, 7–10] The most relevant of these feature tricobalt clusters that are joined by μ_3, η^1 -carbon chains, such as **D** in Figure 1,^[7] or related species with $[(\eta^5\text{-C}_5\text{H}_5)\text{MoCo}_2(\text{CO})_8]$ or $[(\eta^5\text{-C}_5\text{H}_5)\text{WCo}_2(\text{CO})_8]$ endgroups.^[3d] A complex with an $[\text{MnMo}(\mu_2\text{-}\eta^1\text{-C}_2)\text{MnMo}]$ unit has recently been reported (**E**, Figure 1).^[8] Compounds are also known in which two carbons on each end of a (nonlinear) C_x chain are bound to a metal cluster (**F**, Figure 1).^[10]

We began our efforts with cluster endgroups by exploring means of attaching chiral rhenium moieties $[(\eta^5\text{-C}_5\text{Me}_5)\text{Re}(\text{NO})(\text{PPh}_3)\text{C}_x]$ to triosmium carbonyl complexes. This fragment is used extensively in our studies of sp carbon chains

[*] J. A. Gladysz, S. B. Falloon, S. Szafert, A. M. Arif
Department of Chemistry, University of Utah
Salt Lake City, Utah 84112 (USA)
Fax: (+1) 801-581-7808
E-mail: gladysz@rhenium.chemistry.utah.edu

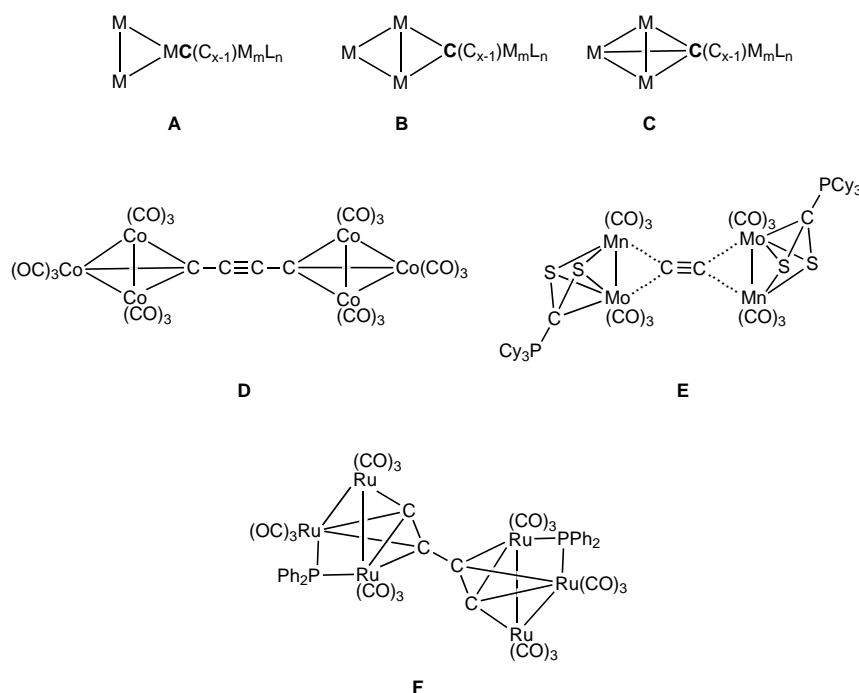
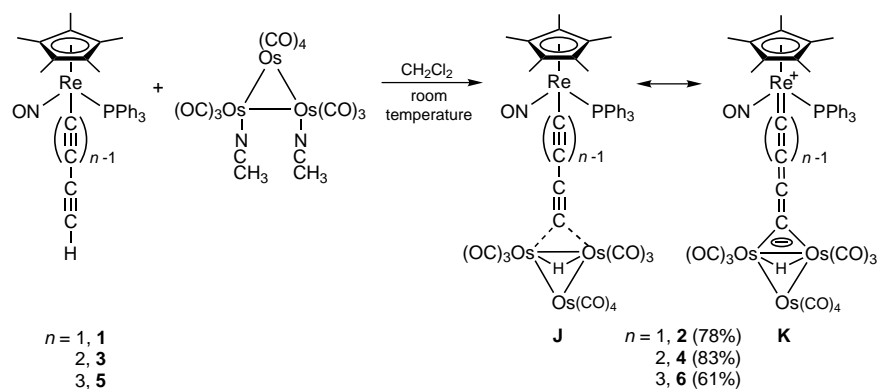


Figure 1. Representative modes of attachment of C_x chains to metal clusters.

with monometallic endgroups, for which $\text{Re}(\text{C}\equiv\text{C})_n\text{Li}$ building blocks are often employed.^[2a,b] In this paper, we report that alkynyl complexes $[(\eta^5\text{-C}_5\text{Me}_5)\text{Re}(\text{NO})(\text{PPh}_3)\{\text{C}\equiv\text{C}\}_n\text{H}]$ can be directly attached to $\text{Os}_3(\text{CO})_{10}$ units to give the title compounds. We also describe the thermal and acid–base properties of these species, and a structurally novel C_3 complex prepared by a complementary route. A portion of this work has been communicated previously.^[11] Companion studies involving complexes with Re/Re_2 and Re/Os_3 termini and bridging C_3OME ligands are reported in detail elsewhere.^[12]

Results

Re(C≡C)_nH-derived complexes: As shown in Scheme 1, the rhenium ethynyl complex $[(\eta^5\text{-C}_5\text{Me}_5)\text{Re}(\text{NO})(\text{PPh}_3)(\text{C}\equiv\text{CH})]$ (**1**)^[13] and triosmium bis(acetonitrile) complex $[\text{Os}_3(\text{CO})_{10}(\text{NCCH}_3)_2]$ were combined in CH_2Cl_2 at room temper-



Scheme 1. Synthesis of $\text{Re}(\text{CC})_n\text{Os}_3$ complexes.

ature. After 3 h, a chromatographic work-up gave an air-stable orange product (**2**, 78%) that was characterized by IR and NMR (^1H , ^{13}C , ^{31}P) spectroscopy as summarized in the Experimental Section. Several observations suggested that **2** had the composition $[(\eta^5\text{-C}_5\text{Me}_5)\text{Re}(\text{NO})(\text{PPh}_3)(\text{CC})\text{Os}_3(\text{CO})_{10}(\text{H})]$. In particular, ^1H and ^{13}C NMR spectra showed a diagnostic hydride ligand signal ($\delta = -16.7$) and ten terminal-CO NMR signals ($\delta = 184\text{--}171$). Spectroscopic evidence for the C_2 unit was sought.

Unsurprisingly, the ReCC ^{13}C NMR signals could not be located unambiguously. Thus, the isotopically labeled complex $\mathbf{2}\text{-}^{13}\text{C}_2$ was prepared analogously from $\mathbf{1}\text{-}^{13}\text{C}_2$.^[2d] Importantly, the ReC ^{13}C signal ($\delta = 245.4$, CD_2Cl_2) was between those of **1** ($\delta = 98.0$, C_6D_6) and the cationic vinylidene complex $[(\eta^5\text{-C}_5\text{Me}_5)\text{Re}(\text{NO})(\text{PPh}_3)(\text{C}=\text{CH}_2)]^+\text{BF}_4^-$ ($\delta = 330.4$, CD_2Cl_2).^[14] The $^2J_{\text{CP}}$ values, which roughly correlate with the rhenium–carbon bond order, were 8.8, 15.8, and 9.5 Hz, respectively. The ReCC ^{13}C NMR signal of $\mathbf{2}\text{-}^{13}\text{C}_2$ ($\delta = 124.2$) was near those of **1** and the vinylidene complex ($\delta = 116.0$, 111.6). However, the $^1J_{\text{CC}}$ value (64.5 Hz) was much less than those of $\mathbf{1}\text{-}^{13}\text{C}_2$ (121 Hz) and the corresponding $\text{ReC}\equiv\text{C}\equiv\text{CRe}$ species (97 Hz), but comparable with that of the analogous $^+\text{Re}=\text{C}=\text{C}=\text{C}=\text{C}=\text{Re}^+$ compound (77 Hz).^[2d]

Similarly, the IR $\tilde{\nu}_{\text{NO}}$ band of **2** (1667 cm^{-1}) was between those of **1** ($1637\text{--}1629\text{ cm}^{-1}$) and the vinylidene complex ($1728\text{--}1711\text{ cm}^{-1}$). The IR spectra of **2** and $\mathbf{2}\text{-}^{13}\text{C}_2$ were also compared. A 1705 cm^{-1} absorption shifted to 1633 cm^{-1} (calcd for $\tilde{\nu}_{^{13}\text{C}^{13}\text{C}}$, 1637 cm^{-1}). The $\tilde{\nu}_{\text{NO}}$ band moved slightly (to 1676 cm^{-1}), but other bands in the $2100\text{--}1600\text{ cm}^{-1}$ region were affected by less than 2 cm^{-1} . Thus, the 1705 cm^{-1} absorption was assigned to the carbon–carbon stretching vibration—a value closer to those associated with double bonds than triple bonds. This and all of the preceding data suggest that the C_2 unit has appreciable $^+\text{Re}=\text{C}=\text{C}$ character.

Many reactions of terminal alkynes and triosmium complexes $[\text{Os}_3(\text{CO})_{10}(\text{L})(\text{L}')]]$ ($\text{L}/\text{L}' = \text{CO}$ or NCCH_3) have been reported.^[15] However, to our knowledge, adducts with formulae analogous to **2** have not been isolated previously. Thus, in order to establish the structure definitively, and to clarify the nature of the C_2 unit, its crystal structure was sought. Accordingly, **2** was crystallized as a hexane hemisolvate. Curiously, all the compounds discussed in this paper showed a marked tendency to retain hexane in the solid state, even after vacuum drying. The structure of **2** was determined as outlined in Table 1 and the Experimental Section.

Table 1. Summary of crystallographic data for **2** · (C₆H₁₄)_{0.5}, **8**⁺SbF₆⁻ · acetone · C₆H₆, and **10** · (C₆H₁₄)_{0.5}.^[a]

	2 · (C ₆ H ₁₄) _{0.5}	8 ⁺ SbF ₆ ⁻ · acetone · C ₆ H ₆	10 · (C ₆ H ₁₄) _{0.5}
formula	C ₄₀ H ₅₁ NO ₁₁ Os ₃ PRE · (C ₆ H ₁₄) _{0.5}	C ₄₀ H ₅₂ F ₆ NO ₁₁ Os ₃ PREsSb · acetone · C ₆ H ₆	C ₄₁ H ₅₃ NO ₁₁ Os ₃ PRE · (C ₆ H ₁₄) _{0.5}
<i>M</i> _r	1531.51	1862.37	1546.54
crystal system	monoclinic	monoclinic	triclinic
space group	<i>P</i> 2 ₁ / <i>n</i>	<i>P</i> 2 ₁ / <i>n</i>	<i>P</i> 1
<i>a</i> [Å]	14.397(4)	15.147(4)	9.575(4)
<i>b</i> [Å]	18.994(3)	21.725(4)	13.909(5)
<i>c</i> [Å]	16.838(2)	17.040(3)	18.937(6)
<i>α</i> [°]			97.92(3)
<i>β</i> [°]	102.78(2)	92.67(2)	103.93(3)
<i>γ</i> [°]			82.93(3)
<i>V</i> [Å ³]	4491(2)	5601(2)	2414(2)
<i>Z</i>	4	4	2
<i>ρ</i> _{calcd} [g cm ⁻³]	2.265	2.208	2.128
<i>ρ</i> _{obs} [g cm ⁻³] (CCl ₄ /CHBr ₂ /CHBr ₂)			2.118–2.122
crystal dimensions [mm]	0.40 × 0.29 × 0.25	0.32 × 0.24 × 0.24	0.32 × 0.22 × 0.09
reflections measured	8212	10205	8038
range/indices (<i>h</i> , <i>k</i> , <i>l</i>)	0 17, 0 22, –20 19	0 17, 0 25, –20 20	0 10, –15 15, –21 21
2 θ limit [°]	2.11 to 24.98	2.07 to 24.97	2.20 to 23.97
observed data, >2 σ (<i>I</i>)	7878	9810	7523
abs. coefficient [mm ⁻¹]	11.24	9.52	10.46
min. transmission [%]	57.7	76.4	42.9
max. transmission [%]	99.9	99.9	99.8
parameters	547	643	532
goodness of fit	1.055	1.043	1.067
<i>R</i> ^[b]	0.0347	0.0378	0.0645
w <i>R</i> ₂ ^[c]	0.0711	0.0788	0.1659
Δ/σ (max)	0.002	0.001	0.008
Δ/ρ (max) [e Å ³]	0.832	0.883	3.464 (1.53 Å from Os2)

[a] Data common to all structures: temperature: 291(2) K; diffractometer: CAD4; radiation: MoK α (0.71073 Å); data collection method: θ -2 θ ; scan speed: variable. [b] $R = \sum ||F_o| - |F_c|| / \sum |F_o|$. [c] $wR_2 = (\sum [w(F_o^2 - F_c^2)]^2) / \sum w[F_o^4]^{1/2}$

Selected bond lengths and angles are given in Table 2, and the molecular structure is depicted in Figure 2 (top). This shows that the ReCC terminus is attached as in **B** (Figure 1), with the hydride ligand bridging the same two osmium atoms. The ReCC group occupies an axial position, as reflected by the near-orthogonality ($\approx 105^\circ$) of the Os₃ and ReOs₂ planes. The rhenium–carbon bond (1.965(9) Å) is shorter than in complexes of formula $[(\eta^5\text{-C}_5\text{Me}_5)\text{Re}(\text{NO})(\text{PPh}_3)(\text{C}\equiv\text{CX})]$ (2.079(9), 2.037(5), 2.032(7) Å),^[2a,c,d] but longer than in similar species with $^+\text{Re}=\text{C}(\text{=C})_n$ linkages (1.909(7), 1.91(1), 1.916(7) Å).^[2d, 4a] Also, the ReC–C bond (1.252(12) Å) is longer than those in disubstituted organic alkynes and alkynyl complexes (mean values 1.192(12) and 1.210(13) Å).^[16] Finally, the P–Re–C41 and C42–Os1–Os3 units are nearly coplanar ($\approx 14.5(5)^\circ$). As illustrated in Figure 3, this can be attributed to the rhenium fragment HOMO in **G**, which would give the idealized conformation **I** for a species with appreciable $^+\text{Re}=\text{C}=\text{C}$ character.^[2d]

Hence, the spectroscopic and structural data show that **2** is best described as a hybrid of the neutral Re–C \equiv C–(Os₃) resonance form **J** and the zwitterionic $^+\text{Re}=\text{C}=\text{C}(\text{Os}_3)^-$ resonance form **K** in Scheme 1. Although formulae such as **J** and **K** see frequent use in the triosmium-cluster literature, it should be emphasized that they can obscure various subtle bonding issues. For example, the coordinatively saturated nature of each osmium atom is more apparent in other representations. Also, resonance form **K** delivers two more electrons to the Os₃ core than **J**, requiring reduced bond orders elsewhere.

Extensions to higher carbon chains were investigated next. As shown in Scheme 1, the reaction of the butadiynyl complex $[(\eta^5\text{-C}_5\text{Me}_5)\text{Re}(\text{NO})(\text{PPh}_3)(\text{C}\equiv\text{CC}\equiv\text{CH})]$ (**3**)^[2a] and $[\text{Os}_3(\text{CO})_{10}(\text{NCCH}_3)_2]$ gave the ReC₄Os₃ adduct $[(\eta^5\text{-C}_5\text{Me}_5)\text{Re}(\text{NO})(\text{PPh}_3)(\text{CCCC})\text{Os}_3(\text{CO})_{10}(\text{H})]$ (**4**) in 83 % yield as a red-orange powder. A low-temperature reaction of the corresponding hexatriynyl complex (**5**)^[2b] afforded the thermally labile ReC₆Os₃ adduct **6** (61 %). However, the analogous octatetraynyl complex $[(\eta^5\text{-C}_5\text{Me}_5)\text{Re}(\text{NO})(\text{PPh}_3)(\text{C}\equiv\text{CC}\equiv\text{C}\equiv\text{CC}\equiv\text{CH})]$ ^[2b] gave a multitude of products.

Mass spectra of **4** and **6** showed intense molecular ion signals, as summarized in the Experimental Section. IR spectra exhibited $\tilde{\nu}_{\text{NO}}$ bands similar to those of **2** (1662 and 1663 cm⁻¹). The ¹H NMR spectra showed upfield OsH signals ($\delta = -13.10$ and -15.90). However, low-temperature ¹³C NMR spectra were complicated by decoalescence phenomena, as often observed with $[(\eta^5\text{-C}_5\text{Me}_5)\text{Re}(\text{NO})(\text{PPh}_3)]$ compounds. Furthermore, practical routes to labeled ¹³C₄ or ¹³C₆ analogues are not available at present. The ReC signals were evident ($\delta = 242.9, 204.9$, brs), but other C_x resonances could only be assigned provisionally.

The UV/Visible spectra of **2**, **4**, and **6** showed several absorption maxima, as summarized in the Experimental Section and illustrated in Figure 4. These were not particularly intense compared with other C_x complexes with $[(\eta^5\text{-C}_5\text{Me}_5)\text{Re}(\text{NO})(\text{PPh}_3)]$ endgroups.^[2, 4] None was significantly solvatochromic (hexane versus CH₂Cl₂ versus CH₃CN). Cyclic voltammograms showed partially reversible oxidations, as summarized Table 3 and illustrated in Figure 4 (inset). A

Table 2. Selected bond lengths [Å] and angles [°] for **2** · (C₆H₁₄)_{0.5}, **8**⁺SbF₆⁻ · acetone · C₆H₆, and **10** · (C₆H₁₄)_{0.5}.

	2 · (C ₆ H ₁₄) _{0.5}	8 ⁺ SbF ₆ ⁻ · acetone · C ₆ H ₆	10 · (C ₆ H ₁₄) _{0.5}
Re–P	2.395(2)	2.402(2)	2.415(4)
Re–N	1.757(7)	1.746(8)	1.728(14)
Re–C41	1.965(9)	1.973(10)	1.96(2)
Re–C1	2.338(9)	2.360(9)	2.32(2)
Re–C2	2.371(9)	2.368(9)	2.30(2)
Re–C3	2.335(9)	2.326(9)	2.36(2)
Re–C4	2.268(9)	2.295(9)	2.38(2)
Re–C5	2.271(9)	2.295(9)	2.34(2)
P–C11	1.831(9)	1.813(10)	1.83(2)
P–C21	1.811(9)	1.824(10)	1.81(2)
P–C31	1.829(9)	1.827(10)	1.86(2)
N–O1	1.186(9)	1.207(9)	1.23(2)
C41–C42	1.252(12)	1.258(12)	1.25(2)
C42–C43	–	–	1.41(3)
Os1–C42	2.150(9)	2.121(9)	2.28(2)
Os3–C42	2.164(9)	2.150(8)	–
Os1–C43	–	–	2.19(2)
Os2–C43	–	–	2.08(2)
Os3–C43	–	–	2.06(2)
Os2–O81 ^[a]	–	–	2.17(2)
Os3–O81 ^[a]	–	–	2.14(2)
Os1–Os3	2.7933(7)	2.8075(8)	2.800(2)
Os1–Os2	2.8728(8)	3.0795(9)	2.822(2)
Os2–Os3	2.8488(7)	2.8463(7)	–
Os1–H1	1.79(9)	1.917(9)	–
Os3–H1	1.82(9)	1.701(9)	–
Os1–H2	–	2.031(9)	–
Os2–H2	–	1.709(9)	–
C–O(av)	1.138	1.147	1.122
N–Re–P	90.5(2)	87.7(3)	88.1(5)
P–Re–C41	94.4(2)	93.5(2)	89.3(4)
N–Re–C41	97.5(3)	99.6(3)	99.3(7)
Re–N–O1	176.6(7)	172.3(7)	170.5(14)
C1–Re–C41	87.3(3)	91.8(4)	96.6(6)
C2–Re–C41	115.4(4)	121.6(4)	130.8(6)
C3–Re–C41	146.9(4)	149.7(4)	148.2(7)
C4–Re–C41	126.9(4)	125.4(4)	116.1(6)
C5–Re–C41	92.4(3)	93.1(3)	90.3(6)
Re–C42–C41	174.2(7)	173.8(7)	178.4(13)
C41–C42–C43	–	–	157.1(18)
C11–P–C21	105.7(5)	105.4(5)	105.7(8)
C11–P–C31	101.0(4)	102.2(4)	105.7(9)
C21–P–C31	103.3(4)	102.8(5)	102.6(8)
Os1–Os3–Os2	61.21(2)	66.00(2)	–
Os1–C42–Os3	80.7(3)	82.2(3)	–
Os2–Os1–Os3	60.349(14)	57.61(2)	72.1(1)
Os1–Os2–Os3	58.44(2)	56.39(2)	–
Os1–C42–C41	139.3(7)	139.4(7)	134.6(14)
Os3–C42–C41	140.0(7)	138.4(7)	–
Os3–Os1–C42	49.9(2)	49.3(2)	72.3(4)
Os2–Os1–C42	81.9(2)	77.5(2)	74.2(5)
Os1–Os3–C42	49.4(2)	48.5(2)	–
Os2–Os3–C42	82.3(2)	82.6(2)	–
C42–Os1–C43	–	–	36.7(7)
Os1–C43–C42	–	–	75.3(11)
Os3–C43–C42	–	–	120.3(13)
Os2–C43–C42	–	–	124.3(13)
Os1–C42–C43	–	–	68.0(9)
Os2–Os1–C43	–	–	47.1(5)
Os3–Os1–C43	–	–	46.8(5)
Os1–Os2–C43	–	–	50.3(5)
Os1–Os3–C41	–	–	50.8(5)
Os1–C43–Os2	–	–	82.6(6)
Os1–C43–Os3	–	–	82.4(6)
Os2–C43–Os3	–	–	106.0(9)
Os2–O81–Os3 ^[a]	–	–	100.3(7)
Os–C–O(av)	178.2	177.3	176.2

[a] Os2–O81' = 1.90(2); Os3–O81' = 2.25(2); Os2–O81'–Os3 = 105.5(10)

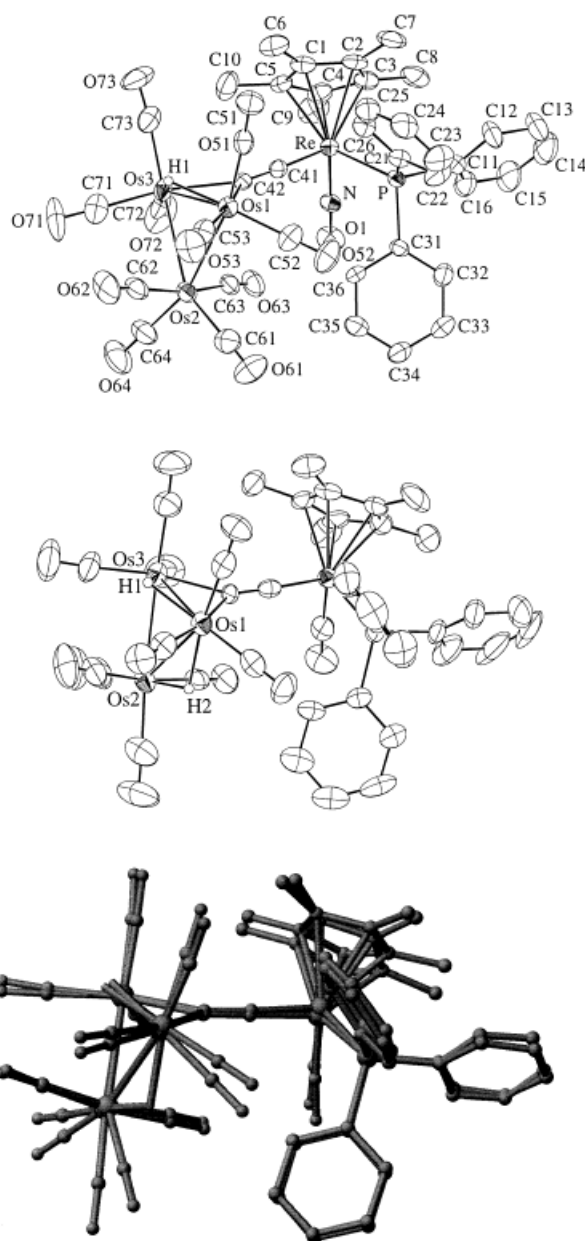


Figure 2. Structures of **2** · (C₆H₁₄)_{0.5} (top) and the cation of **8**⁺ · SbF₆⁻ · acetone · C₆H₆ (middle), and a superposition (bottom).

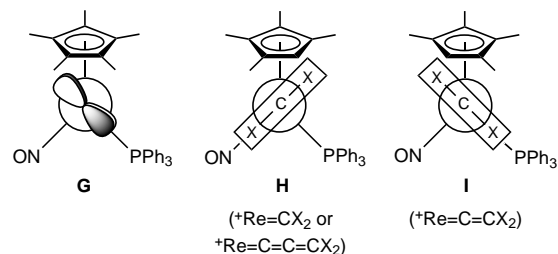


Figure 3. Relationship between the HOMO of [(η^5 -C₅Me₅)Re(NO)(PPh₃)]⁺ (**G**) and conformations of ⁺Re=C species.

more positive E^\ominus value indicates a thermodynamically less favorable oxidation. These data are further analyzed below.

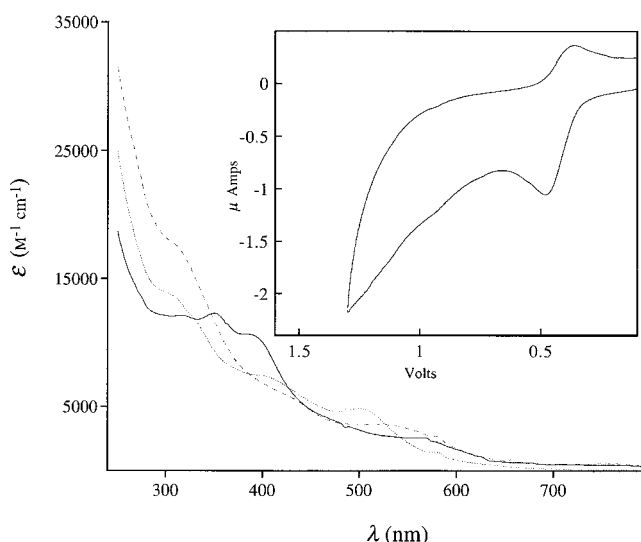


Figure 4. UV–Visible spectra of **2** (full line), **4** (dotted line), **6** (broken line); hexane, ambient temperature), and (inset) cyclic voltammogram of **4** at 100 mV s⁻¹ (0.1M *n*-Bu₄N⁺BF₄⁻/CH₂Cl₂; E⁰(ferrocene) = 0.46).^[24]

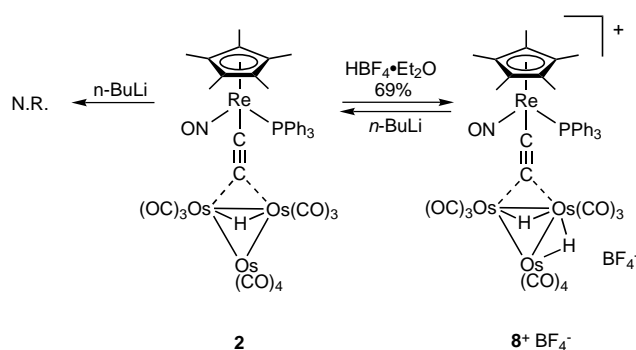
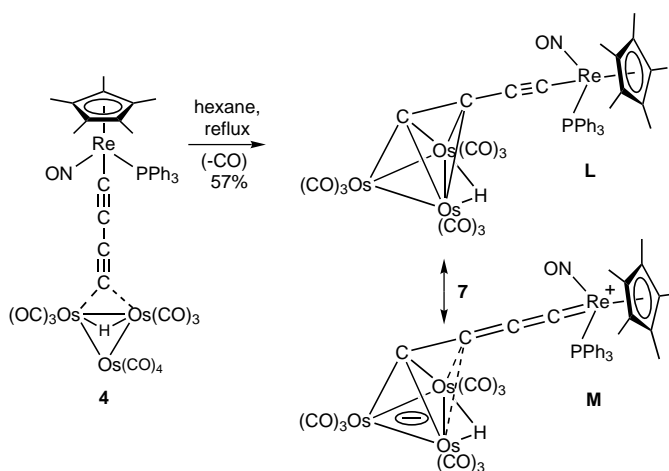
Table 3. Cyclic voltammetry data.^[a]

	<i>E</i> _{p,a} [V]	<i>E</i> _{p,c} [V]	<i>E</i> ⁰ [V]	<i>i</i> _{ca}
2	0.87	0.68	0.78	≪ 1
4	0.47	0.38	0.43	< 1
6	0.50	0.38	0.44	< 1
[Os ₃ (CO) ₁₂]	–	–	–	–
[Os ₃ (CO) ₁₀ (CH ₃ CN) ₂]	0.83	–	–	∞

[a] 7–9 × 10⁻⁵ M in 0.1M *n*-Bu₄N⁺BF₄⁻/CH₂Cl₂ at 22.5 ± 1 °C; Pt working and counter electrodes, Ag wire pseudoreference electrode, ferrocene standard as in ref. [24]; scan rate 100 mV s⁻¹.

Reactions of Re(CC)_nOs₃ complexes: The stabilities of **2**, **4**, and **6** decreased with increasing chain length, both in solution and in the solid state (decomp 210–213, 107–110, 65–66 °C). We probed the nature of these decomposition pathways. When **2** was refluxed for several hours in nonane or decane, little reaction occurred. When **4** was refluxed in hexane, a clean transformation took place (Scheme 2). Workup gave a nonacarbonyl complex with the composition [(η⁵-C₅Me₅)Re(NO)(PPh₃)(CCCC)Os₃(CO)₉(H)] (**7**) in 57% yield, as evidenced by mass spectrometry and microanalysis. The ¹H and ¹³C NMR spectra showed diagnostic OsH (δ = -22.34) and ReC (δ = 242.9, d, J_{CP} = 11.5 Hz) signals. A structure consistent with these data is given in Scheme 2.

Attempts to grow crystals of **7** suitable for X-ray analysis were unsuccessful. However, analogous adducts of Os₃(CO)₉(H) and ligands of the formula CCR (R = H, CH₃, etc.) had been characterized previously.^[15, 17] All exhibit OsH ¹H NMR signals near δ = -23, and IR $\tilde{\nu}_{\text{CO}}$ patterns similar to **7**. As described below, Bruce has isolated closely related triruthenium complexes.^[3b, 18] Hence, the structure in Scheme 2 is highly probable. Also, **7** gave an IR $\tilde{\nu}_{\text{NO}}$ band (1663 cm⁻¹) near those of **2**, **4**, and **6**. Together with the ReC ¹³C NMR data and reference values given above, this suggests an appreciable contribution by the zwitterionic resonance form **M** in Scheme 2.



Scheme 2. Reactions of Re(CC)_nOs₃ complexes.

When **4** was refluxed in tetrahydrofuran (THF) with phosphines such as PPh₃ or PMe₂Ph substitution occurred. However, several species were formed and could not be separated or purified. We therefore turned our attention to the acid–base properties of these compounds. For example, we wondered whether the hydride ligands might be abstracted to give anions that could be alkylated or otherwise functionalized. Thus, **2** and *n*-BuLi (1 equiv) were combined in CD₂Cl₂ at -80 °C. No reaction occurred, as assayed by ¹H and ³¹P NMR. The sample was warmed to room temperature, and *n*-BuLi (9 equiv) was added. Only **2** was detected. Similarly, **2** and *n*-BuLi (10 equiv) did not react in C₆D₆ at room temperature. Since this suggested a very electron-rich triosmium system, protonations were then attempted.

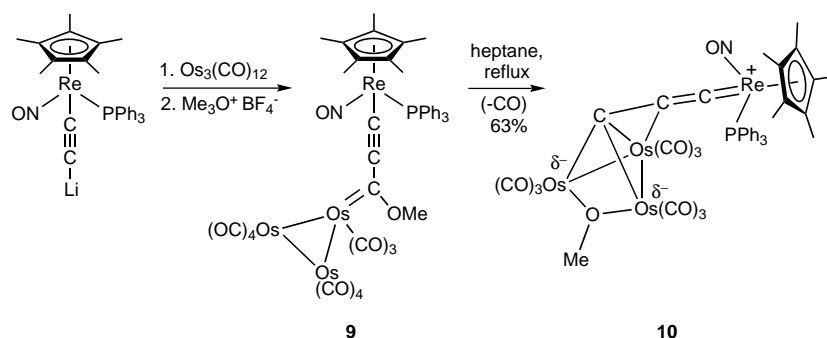
As illustrated in Scheme 2, **2** and HBF₄·Et₂O (1 equiv) were combined in CD₂Cl₂. A ¹H NMR spectrum showed clean conversion to a new compound that exhibited two upfield OsH signals (δ = -15.68, -19.39, 2d, J_{HH} = 0.9 Hz). Workup gave the cationic dihydride complex [(η⁵-C₅Me₅)Re(NO)(PPh₃)(CC)Os₃(CO)₁₀(H)₂]⁺ BF₄⁻ (**8**⁺ BF₄⁻) as an orange powder in 69% yield. The $\tilde{\nu}_{\text{NO}}$ value (1674 cm⁻¹) indicated an appreciable contribution by a ⁺Re=C=C(Os₃) resonance form, which in contrast to the case of **2** is cationic as opposed to zwitterionic. A CD₂Cl₂ solution of **8**⁺ BF₄⁻ was treated with 1.0 equiv of *n*-BuLi at room temperature. A ¹H NMR spectrum showed the clean regeneration of **2**.

A sample of $\mathbf{8}^+\text{BF}_4^-$ was treated with NaSbF_6 . Crystallization yielded the hexafluoroantimonate salt $\mathbf{8}^+\text{SbF}_6^-$ as an acetone· C_6H_6 solvate. The structure was determined as described Table 1 and the Experimental Section. The cation is depicted in Figure 2 (middle), and key bond lengths and angles are summarized in Table 2. The rhenium–carbon and $\text{ReC}–\text{C}$ bond lengths (1.973(10), 1.258(12) Å) are essentially identical with those of **2**. The P–Re–C41 and C42–Os1–Os3 planes also define an angle very close to that in **2** (10.6(6) $^\circ$ versus 14.5(5) $^\circ$). As shown by the overlay in Figure 2 (bottom), the only significant difference involves the disposition of carbonyl ligands on the osmium atoms bridged by the new hydride ligand. Nearly all other bond lengths and angles are within experimental error (that is, within three esd values) of each other (Table 2).

Re(C₃OMe)Os₃-derived complexes: We recently reported the synthesis of the C₃OMe complex $[(\eta^5\text{-C}_5\text{Me}_5)\text{Re}(\text{NO})(\text{PPh}_3)(\text{C}=\text{CC}(\text{OMe})=\text{Os}_3(\text{CO})_{11})]$ (**9**) by the route sketched in Scheme 3.^[12] This constitutes another approach to attaching $[(\eta^5\text{-C}_5\text{Me}_5)\text{Re}(\text{NO})(\text{PPh}_3)\text{C}_x]$ moieties to triosmium carbonyl clusters. Unfortunately, BF_3 gas did not abstract the methoxide group cleanly,^[12] despite successes with related complexes with monometallic termini.^[4] However, we thought that **9** might give novel ReC_3Os_3 species under other conditions, so thermolyses were investigated.

As shown in Scheme 3, a heptane solution of **9** was refluxed. Workup gave a red-orange powder (**10**) in 63% yield, and prisms of a hexane hemisolvate were obtained from $\text{CH}_2\text{Cl}_2/\text{hexane}$. These were of borderline quality for X-ray crystallography. However, NMR spectra showed several perplexing phenomena (see below), and a structure could not be confidently assigned. Thus, a data set was collected analogously to those above. Refinement revealed a methoxy ligand bridging two osmium atoms, and an apparent disorder associated with the oxygen (62(4):38(4) occupancy). In view of a lack of precedent for certain features of the minor form, several points should be emphasized here.

First, the mass spectrum suggested that **10** was derived from the loss of two CO ligands from **9**, and the microanalysis (see Experimental Section) was in excellent agreement with a hexane hemisolvate of this formula. Second, the ^1H NMR spectrum verified the hexane hemisolvate, and showed no OsH signals ($\delta = 0$ to -22). Third, the density determined by flotation was very close to the crystallographic density



Scheme 3. Synthesis of an ReC_3Os_3 complex with a carbon more distorted than planar tetracoordinate.

(Table 1; 2.068 g cm^{-3} without hexane). Fourth, the prisms melted without decomposition at $172–174\text{ }^\circ\text{C}$, and remelted at $170–173\text{ }^\circ\text{C}$, consistent with a homogeneous compound. Fifth, the isotope envelope of the molecular ion closely matched calculated ratios, as illustrated in Figure 5. In summary, there is no evidence for a contaminant ligand that either accompanies or replaces the bridging methoxy ligand.

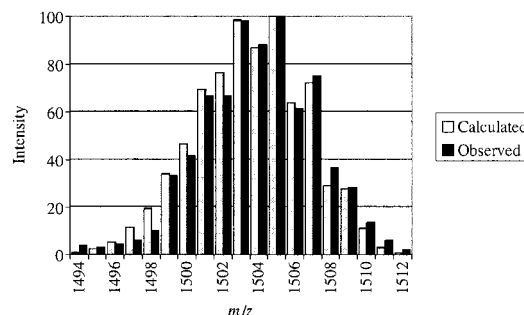


Figure 5. Comparison of observed and calculated isotope patterns for the molecular ion of **10**.

The major form of **10** is depicted in Figure 6 (top), and both forms are filed in the Supplementary Information (see under Crystallography, below). Most importantly, **10** is indeed an unusual ReC_3Os_3 complex, in which the ReCCC terminus bridges all three osmium atoms and the central carbon is bound to the only osmium that is not methoxide-bridged. The mode of chain attachment is related to, but not identical with, that in **F** (Figure 1). The partial structure **N** (Figure 6) illustrates pseudosymmetries ($\text{Os}_2 \approx \text{Os}_3$) that are less apparent in other representations. Rotations of **N** by $\pm 90^\circ$ yield the partial structures **O** and **P**. These highlight the unusual geometry about C43, which is analyzed further below. Unfortunately, the ^{13}C NMR signals of the ReC_3Os_3 unit could not be located.

The Cambridge Crystallographic Database contains many triosmium clusters with bridging methoxy ligands. All show nearly equal osmium–oxygen bonds that occupy converging octahedral coordination sites, as found for the major form of **10** ($\text{Os}_2\text{–O81}$ 2.17(2), $\text{Os}_3\text{–O81}$ 2.14(2) Å).^[19] No cases of disorder have been reported. The minor form of **10** exhibits very different osmium–oxygen bond lengths ($\text{Os}_2\text{–O81}'$ 1.90(2), $\text{Os}_3\text{–O81}'$ 2.25(2) Å), with the oxygen significantly removed from the converging octahedral coordination sites.

After much careful study, we have been unable to explain these properties or identify an artifactual origin. Rather than pursue an open-ended and possibly unresolvable problem further, we simply focus for the remainder of this paper on the logical data associated with the major form of **10**.

We analyze the bonding in **10** as follows. First, the rhenium–carbon bond length (1.96(2) Å) and IR $\tilde{\nu}_{\text{NO}}$ value (1668 cm^{-1}) indicate about the same degree of $^+\text{Re}=\text{C}=\text{C}$ character as in the even-carbon $\text{Re}(\text{CC})_n\text{Os}_3$ compounds. Second, it should be noted that if a metal were to coordinate the terminal

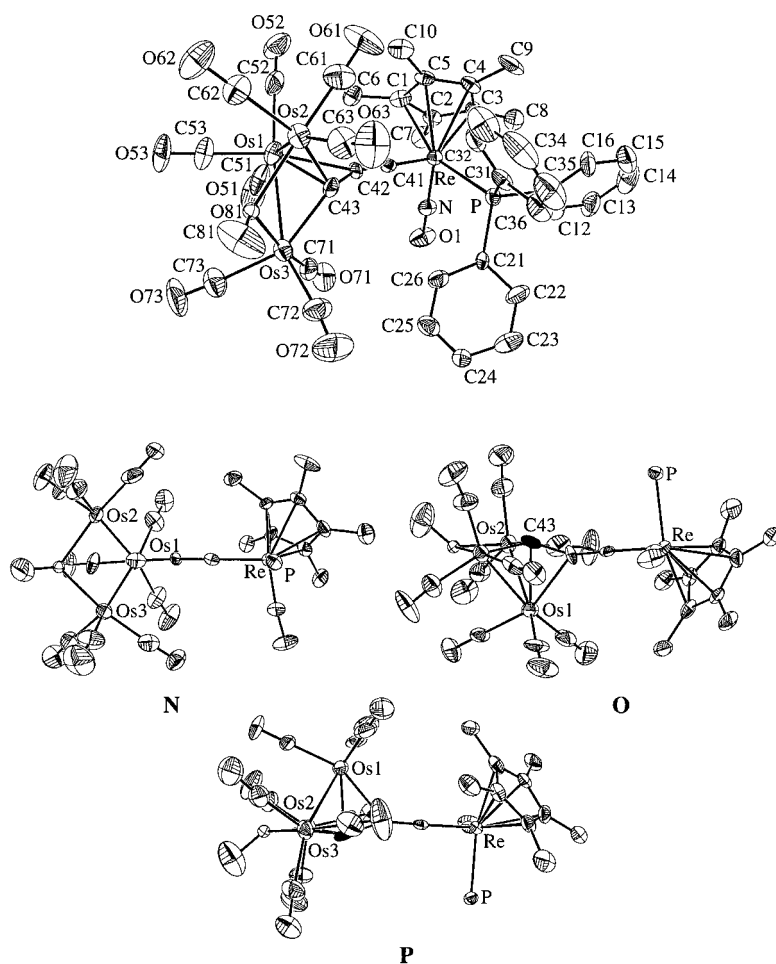


Figure 6. Structure of major form of **10** (C_6H_{14})_{0.5} (top), and partial views (middle, bottom).

C=C linkage of an $+Re=C=C=CX_2$ species (**H**, Figure 3), it must bind either *anti* or *syn* to the rhenium–phosphorus bond. Both modes would give coplanar P–Re–C and C–C–M moieties. As is evident in Figure 6 (top), the P–Re–C41 and C42–C43–Os1 units of **10** are nearly coplanar ($\sphericalangle 3.1(5)^\circ$) with Os1 *anti* to the Re–P bond. Thus, **10** can be viewed as an osmium π complex of an $+Re=C=C=C(Os_2)$ linkage. The usual rehybridization is evident, as reflected by the C41–C42–C43 bond angle ($157.1(18)^\circ$). Overall, the ReC_3 moiety constitutes a five-electron, $2\pi/3\sigma$, $+Re=C=C=C:$ donor.

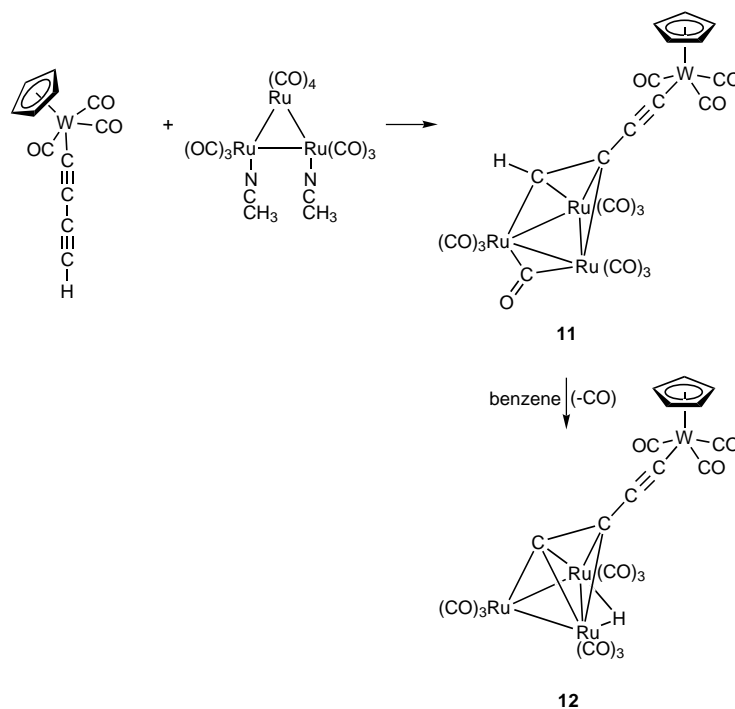
As a final complexity, NMR spectra of **10** reveal more than one isomer in solution. Ratios are markedly solvent-dependent. In CD_2Cl_2 , crystallized samples show two methoxy and two pentamethylcyclopentadienyl 1H signals in 48:52 area ratios ($\delta = 3.79, 3.51$ and $1.76, 1.72$).^[20] We propose that these represent geometric isomers about the $+Re=C$ linkage, as previously observed for **H** and **I** (Figure 3) in cases of unequivalent X groups. For example, the methylvinylidene complex $[(\eta^5-C_5Me_5)Re(NO)(PPh_3)(=C=CHCH_3)]^+ BF_4^-$ gives a 57:43 equilibrium mixture of isomers.^[13] With **10**, this exchanges Os1 and C43, or the $+Re=C=C=C(Os_2)$ face to which Os1

coordinates. Curiously, three ^{31}P signals were reproducibly observed ($\delta = 23.6, 22.0, 21.6$; area ratio 52.6:19.7:27.7). The two less intense peaks presumably correspond to additional isomers of one of the $+R=C$ isomers.^[21]

Discussion

Many reactions of terminal alkynes and triosmium complexes $[Os_3(CO)_{10}(L)(L')]$ ($L, L' = CO$ or $NCCH_3$), as well as triiron and triruthenium analogues, have been reported.^[15] Surprisingly, to our knowledge no adducts analogous to the $Re(CC)_nOs_3$ species **2**, **4**, or **6** have been described previously. Recently, reactions of terminal alkynes and a low-temperature $Ru_3(CO)_{11}$ source have been shown to give the π adducts $[Ru_3(CO)_{11}(\eta^2-R_2C=CH)]$.^[22] Although there are several modes by which **1**, **3**, or **5** might initially interact with $[Os_3(CO)_{10}(NCCH_3)_2]$ in Scheme 1, this provides a precedent for the simplest possibility.

As shown in Scheme 4, Bruce et al. have found that the tungsten butadiynyl complex $[(\eta^5-C_5H_5)W(CO)_3(C\equiv C\equiv CH)]$ and triruthenium species $[Ru_3(CO)_{10}(NCCH_3)_2]$ react to give **11**, which has a $\mu_3, \eta^2-C\equiv CH$ moiety.^[18] When refluxed in benzene, **11** decarbonylates to the $WC_4Ru_3(CO)_9(H)$ complex **12**, which is analogous to the $ReC_4Os_3(CO)_9(H)$ complex **7** obtained by the thermolysis of **4** in Scheme 1. In principle, a tungsten/triruthenium complex sim-



Scheme 4. Synthesis of a WC_4Ru_3 complex.

ilar to **4** might be on the reaction coordinate between **11** and **12**. Alternatively, a rhenium/triosmium complex similar to **11** might be on the reaction coordinate leading to **4**. However, no intermediates were detected by ^{31}P NMR under the conditions of Scheme 1.^[23]

The spectroscopic features of our new complexes have close precedents in related rhenium or triosmium species. However, the oxidations of **2**, **4**, and **6** (Table 3 and Figure 4) have no counterparts in $[\text{Os}_3(\text{CO})_{10}(\text{L})_2]$ compounds, and the potentials are much less favorable thermodynamically than those of other $[(\eta^5\text{-C}_5\text{Me}_5)\text{Re}(\text{NO})(\text{PPh}_3)(\text{C}\equiv\text{CX})]$ systems ($\text{R} = \text{Pd}(\text{PEt}_3)_2\text{Cl}$, $\text{C}\equiv\text{CPd}(\text{PEt}_3)_2\text{Cl}$, $\text{C}\equiv\text{CRe}(\text{NO})(\text{PPh}_3)(\eta^5\text{-C}_5\text{Me}_5)$, $E^\ominus(\text{CH}_2\text{Cl}_2)^{[24]} = -0.02, 0.22, 0.01$).^[2] One rationale would be a greater contribution by zwitterionic resonance forms $^+\text{Re}=(\text{C}=\text{C})_n=(\text{Os}_3)^-$. This would explain the less facile oxidation versus other rhenium complexes, or the more facile oxidation versus other triosmium complexes. In contrast to symmetrical $\text{Re}(\text{CC})_n\text{Re}$ complexes,^[2b] the longer-chain adducts **4** and **6** are more easily oxidized than **2**. This would be rationalized by a slight decrease in zwitterionic character with chain length, rendering the rhenium more electron-rich, which is consistent with the modest trend in IR $\tilde{\nu}_{\text{NO}}$ values (**2/4/6**, 1667/1662/1663 cm^{-1}).

Numerous mechanistic possibilities exist for the generation of **10** in Scheme 3. We suggest that an initial carbon monoxide dissociation is followed by a nucleophilic attack of the $\text{ReC}\equiv\text{C}$ carbon upon the triosmium core, and then methoxide migration. We are aware of only one other adduct of $[\text{Os}_3(\text{CO})_9(\text{OMe})]$ and a five-electron donor ligand, an $[\text{Me}_2\text{NCC}(\text{H})=\text{CR}]$ complex reported by Adams.^[19a] The most unusual feature of **10** is emphasized in views **O** and **P** in Figure 6, namely that all of the bonds to the tetracoordinate ReCCC terminus (C43) are directed to one side of a spatial plane. Such deformations are even more severe than that of planar tetracoordinate carbon,^[25, 26] and should introduce considerable strain and reactivity.

In fact, C43 is better described as having a trigonal bipyramidal geometry with Os1 as one axial substituent and the other axial substituent missing. The assembly is umbrella-like, with the three equatorial substituents (Os2, Os3, C42) slightly bent towards the Os1 handle. The deviation from the equatorial plane is reflected in the sum of the C42-C43-Os2, C42-C43-Os3, and Os2-C43-Os3 bond angles (350.6°). Similar situations occur with small-ring propellanes, in which the quaternary carbons are said to have inverted geometries.^[27] It is noteworthy that Os1 is bound to the other three substituents of C43, analogously to η^4 -trimethylenemethane complexes.^[28] Since osmium-carbon bonds are intrinsically shorter than osmium-osmium bonds, the angle of the Os1-C43 bond with the Os2-Os3-C42 plane (65.2°) is less than 90° .

There is a growing awareness that cluster-based C_x complexes, and other types of organometallic species, can contain carbons with highly distorted geometries.^[12, 26b,c, 28] Although **7** and **12** have not yet been structurally characterized, the four bonds to their MCCCC termini must also lie on one side of a spatial plane. Importantly, Shriver et al. have shown that unique reactivity modes can be associated with such carbons.^[6a, 29] However, the chemistry of these highly deformed

systems remains underexplored and constitutes an ongoing objective of our program.

We have not attempted in this paper to review all of the modes by which elemental carbon chains can bind to metal clusters. However, the samples in Figure 1, coupled with our data and the other examples cited, presage a field that will become increasingly systematized. These efforts will be motivated in part by practical objectives. For example, two-dimensional superlattices of alkynyl- and aryl-linked metal clusters are under active pursuit in other laboratories, with the ultimate aim of producing nanoelectronic digital circuits.^[30] Finally, there are increasing numbers of polymetallic arrays in which ligands are joined by sp-carbon chains.^[31]

In summary, we have demonstrated that even-membered sp-carbon chains with monorhenium and $\text{Os}_3(\text{CO})_{10}(\text{H})$ endgroups are easily constructed. The resulting η^1, μ_2 assemblies are labile. From some standpoints this is desirable, as other architecturally interesting carbon complexes such as **7** (or from related precursors, **10**) can be readily accessed. However, from a perspective of long-lived structures or molecular devices, this is undesirable. Hence, one productive direction for future research would be trimetallic systems with less-dissociable spectator ligands, a more restricted set of binding modes, and higher kinetic barriers. Nevertheless, the new ReC_xOs_3 complexes described above have interesting properties in their own right, and will be the subject of ongoing investigations.

Experimental Section

General data: General procedures and instrumentation have been described previously.^[2a] Cyclic voltammograms were recorded with new protocols.^[2d, 24] The CH_2Cl_2 and CD_2Cl_2 were distilled or vacuum-transferred from CaH_2 , and THF and hexane were distilled from K/benzophenone. Other solvents or reagents were used as received from commercial suppliers.

$(\eta^5\text{-C}_5\text{Me}_5)\text{Re}(\text{NO})(\text{PPh}_3)(\text{CC})\text{Os}_3(\text{CO})_{10}(\text{H})$ (2**):** A Schlenk flask was charged with **1**^[22] (0.025 g, 0.039 mmol), $[\text{Os}_3(\text{CO})_{10}(\text{NCCCH}_3)_2]$ (0.037 g, 0.039 mmol)^[33] and CH_2Cl_2 (10 mL). The mixture was stirred for 3 h. Solvent was removed under vacuum (oil-pump). Thin-layer chromatography (silica gel; hexane/ CH_2Cl_2 , 2:1 v/v) gave an orange band, which was extracted with CH_2Cl_2 . The extract was concentrated (approx. 1 mL), and hexane was added (10 mL). Solvent was removed under vacuum (oil-pump) to give **2** as an orange powder retaining 0.4–0.5 equiv hexane (0.047 g, 0.031 mmol, 78 %).^[34a] A CH_2Cl_2 solution of **2** was layered with hexane in a sealed vial. This gave orange-red prisms that were used for X-ray crystallography, m.p. 210–213 $^\circ\text{C}$ (decomp). $\text{C}_{40}\text{H}_{31}\text{NO}_{11}\text{Os}_3\text{PRE}\cdot(\text{C}_6\text{H}_{14})_{0.5}$; calcd C 33.71, H 2.41; found C 33.03, H 2.35; IR (hexane): $\tilde{\nu} = 2091$ (m), 2054 (s), 2039 (m), 2005 (vs), 1981 (m, sh), 1969 (m), 1705 (m), 1667 cm^{-1} (m); ^1H NMR (CD_2Cl_2): $\delta = 7.99, 7.40, 7.26$ (m, 3Ph), 1.74 (s, C_5Me_5), -16.70 (s, OsH);^[34a] $^{13}\text{C}\{^1\text{H}\}$ NMR (CD_2Cl_2): $\delta = 183.9, 183.8, 182.7, 181.8, 179.3, 178.4, 175.3, 172.8, 172.4, 170.7$ (s, 10 CO), 135.7 (brd, *o*-Ph), 132.1 (brd, *i*-Ph), 129.3 (s, *p*-Ph), 128.5 (brd, *m*-Ph), 104.8 (s, $\text{C}_5(\text{CH}_3)_5$), 10.2 (s, $\text{C}_5(\text{CH}_3)_5$); $^{31}\text{P}\{^1\text{H}\}$ NMR (CD_2Cl_2): $\delta = 21.0$ (s); UV/Vis (1.1×10^{-5} M; hexane): $\lambda_{\text{max}}(\epsilon) = 316$ (1.2×10^4), 350 (1.2×10^4), 384 nm (1.1×10^4); (CH_2Cl_2): $\lambda_{\text{max}}(\epsilon) = 320$ (1.9×10^4), 342 (1.8×10^4), 390 nm (1.4×10^4); (CH_3CN): $\lambda_{\text{max}}(\epsilon) = 318$ (1.8×10^4), 342 (1.7×10^4), 394 nm (1.3×10^4).

$(\eta^5\text{-C}_5\text{Me}_5)\text{Re}(\text{NO})(\text{PPh}_3)(^{13}\text{C}^{13}\text{C})\text{Os}_3(\text{CO})_{10}(\text{H})$ (2**- $^{13}\text{C}_2$):** This complex was prepared from **1**- $^{13}\text{C}_2$ ^[2d] by a procedure analogous to that for **2**, m.p. 210–213 $^\circ\text{C}$ (decomp). IR (hexane): $\tilde{\nu} = 2091$ (m), 2054 (s), 2041 (m), 2006 (vs), 1980 (m), 1968 (m), 1676 (m), 1633 cm^{-1} (m); ^1H NMR (CD_2Cl_2): $\delta = 7.47$ (m, 3Ph), 1.73 (s, C_5Me_5), -16.71 (s, OsH);^[34a] $^{13}\text{C}\{^1\text{H}\}$ NMR (CD_2Cl_2):

$\delta = 245.4$ (dd, $J_{CP} = 8.8$ Hz, $J_{CC} = 64.5$ Hz, ReC), 183.9, 183.8, 182.8, 181.9, 179.4, 178.4, 175.3, 172.8, 172.4, 170.7 (s, 10 CO), 135.6 (brd, *o*-Ph), 132.1 (brd, *i*-Ph), 129.3 (s, *p*-Ph), 128.5 (brd, *m*-Ph), 124.2 (d, $J_{CC} = 64.5$ Hz, ReCC), 104.8 (s, $C_5(CH_3)_5$), 10.2 (s, $C_5(CH_3)_5$); $^{31}P\{^1H\}$ NMR (CD_2Cl_2): $\delta = 20.6$ (d, $J_{PC} = 8.9$ Hz).

[(η^5 -C₅Me₅)Re(NO)(PPh₃)(CCCC)Os₃(CO)₁₀(H)] (4): A Schlenk flask was charged with **3**^[2a] (0.020 g, 0.030 mmol), [Os₃(CO)₁₀(NCCH₃)₂] (0.028 g, 0.031 mmol), and CH₂Cl₂ (10 mL). The mixture was stirred for 3 h. Solvent was removed under vacuum (oil-pump). The residue was dissolved in CH₂Cl₂ (1 mL), and hexane (10 mL) was added. The precipitate was collected by filtration and dried under vacuum (oil-pump) to give **4** as a red-orange powder retaining approximately 0.25 equiv of hexane (0.038 g, 0.025 mmol, 83 %),^[34b] m.p. 107–110 °C (decomp); IR (hexane): $\tilde{\nu} = 2093$ (m), 2057 (vs), 2043 (vs), 2017 (vs), 2001 (vs), 1662 cm⁻¹ (m); 1H NMR ($CDCl_3$): $\delta = 7.41$ –7.39 (m, 3 Ph), 1.76 (s, C₅Me₅), -13.10 (s, OsH);^[34b] $^{13}C\{^1H\}$ NMR (CD_2Cl_2): $\delta = 178.4$ (s), 153.4 (s), 145.8 (s), 139.2 (s), 139.0 (s), 134.5 (d, $J_{CP} = 10.3$ Hz, *o*-Ph), 130.7 (s, *p*-Ph), 128.7 (d, $J_{CP} = 10.4$ Hz, *m*-Ph), 102.0 (s, C₅(CH₃)₅), 10.4 (s, C₅(CH₃)₅); $^{31}P\{^1H\}$ NMR (CD_2Cl_2 , -80 °C): $\delta = 242.9$ (br, ReC), 187.7, 185.7, 182.6, 181.6, 180.4, 179.0, 177.5, 175.8, 174.3, 174.2 (s, 10 CO), 152.6, 148.4, 144.7 (s, ReCCCC), 138.2–127.7 (3 C₆H₅), 101.1 (s, C₅(CH₃)₅), 9.82 (s, C₅(CH₃)₅); $^{31}P\{^1H\}$ NMR (CD_2Cl_2): $\delta = 21.6$ (s); UV/Vis (1.7×10^{-5} M, hexane): 296 (1.4×10^4), 388 (7.5×10^3), 500 nm (4.9×10^3); (CH_2Cl_2): λ_{max} (ϵ) = 296 (sh, 1.9×10^4), 508 nm (5.7×10^3); (CH_3CN): λ_{max} (ϵ) = 298 (1.9×10^4), 506 nm (6.2×10^3); MS (positive Cs-FAB, 3-NBA/CH₂Cl₂):^[35] m/z : 1514 [4^+] (40 %), 1486 [$4^+ - CO$] (100 %), 614 [(η^5 -C₅Me₅)Re(NO)(PPh₃)⁺] (35 %), no other peaks > 15 % at $m/z > 450$.

[(η^5 -C₅Me₅)Re(NO)(PPh₃)(CCCC)Os₃(CO)₁₀(H)] (6): A Schlenk flask was charged with **5**^[2b] (0.025 g, 0.036 mmol) and [Os₃(CO)₁₀(NCCH₃)₂] (0.034 g, 0.036 mmol) and cooled to -45 °C (NCCH₃/CO₂). The solution was stirred and CH₂Cl₂ (10 mL) was added. The cold bath was allowed to warm to room temperature. After 2 h, hexane (10 mL) was added. The mixture was filtered through Celite (2 cm plug). Solvent was removed from the filtrate under vacuum (oil-pump) to give **6** as a red-brown powder retaining approximately 0.6 equiv of hexane (0.035 g, 0.023 mmol, 61 %),^[34c] decomp (no melting) at 65–66 °C. C₄₄H₃₁NO₁₁Os₃PRE · (C₆H₁₄)_{0.5}: calcd C 34.95, H 2.40; found C 34.94, H 2.43; IR (hexane): $\tilde{\nu} = 2095$ (w), 2060 (vs), 2043 (sh), 2025 (vs), 2004 (vs), 1843 (w), 1663 cm⁻¹ (w); 1H NMR (CD_2Cl_2): $\delta = 7.48$ –7.40 (m, 3 Ph), 1.71 (s, C₅Me₅), -15.90 (s, OsH);^[34c] $^{13}C\{^1H\}$ NMR (CD_2Cl_2 , partial): $\delta = 133.5$ (d, $J_{CP} = 10.2$ Hz, *o*-Ph), 129.9 (s, *p*-Ph), 127.8 (d, $J_{CP} = 10.2$ Hz, *m*-Ph), 100.7 (s, C₅(CH₃)₅), 9.3 (s, C₅(CH₃)₅); $^{13}C\{^1H\}$ NMR (CD_2Cl_2 , -80 °C): $\delta = 204.9$ (br, ReC), 190.5, 187.7, 186.9, 185.6, 183.3, 179.3, 177.5, 175.0, 174.3, 173.9 (s, 10 CO), 137.7, 136.9 (s, 2 C of ReCCCC),^[36] 134.7–127.9 (3 C₆H₅), 113.1, 112.6, 109.4 (s, 3 C of ReCCCC),^[36] 100.7 (s, C₅(CH₃)₅), 9.6 (s, C₅(CH₃)₅); $^{31}P\{^1H\}$ NMR (CD_2Cl_2): $\delta = 22.3$ (s); UV/Vis (1.1×10^{-5} M, hexane): λ_{max} (ϵ) = 306 (1.8×10^4), 516 nm (3.6×10^3); (CH_2Cl_2): λ_{max} (ϵ) = 306 (2.1×10^4), 516 nm (4.1×10^3); MS (positive Cs-FAB, 2-nitrophenyl octyl ether/CH₂Cl₂):^[35] m/z : 1538 [6^+] (100 %), 1510 [$6^+ - CO$] (40 %), no other peaks > 20 % at $m/z > 500$.

[(η^5 -C₅Me₅)Re(NO)(PPh₃)(CCCC)Os₃(CO)₉(H)] (7): A Schlenk flask was charged with **4** (0.023 g, 0.015 mmol) and hexane (15 mL) and fitted with a condenser. The solution was refluxed and stirred (2 h), and then cooled to room temperature. The solvent was decanted from a residue and removed under vacuum (oil-pump) to give **7** as a red-brown powder retaining approximately 0.4 equiv of hexane (0.013 g, 0.008 mmol, 57 %),^[34d] decomp (no melting) 87–89 °C. C₄₁H₃₁NO₁₀Os₃PRE · (C₆H₁₄)_{0.5}: calcd C 33.79, H 2.41; found C 33.71, H 2.41; IR (CH_2Cl_2): $\tilde{\nu} = 2095$ (w), 2070 (vs), 2047 (s), 2037 (m), 2023 (sh), 2014 (vs), 1975 (m), 1663 cm⁻¹ (w); 1H NMR (CD_2Cl_2): $\delta = 7.49$ –7.41 (m, 3 Ph), 1.77 (s, C₅Me₅), -22.34 (s, OsH);^[34d] $^{13}C\{^1H\}$ NMR ([D₈]THF): $\delta = 174.9$ (s), 170.2 (s), 170.1 (s), 166.0 (s), 134.4 (d, $J_{CP} = 10.7$ Hz), 132.5 (d, $J_{CP} = 9.8$ Hz), 130.9 (s, *p*-Ph), 128.9 (d, $J_{CP} = 10.5$ Hz, *m*-Ph), 102.0 (s, C₅(CH₃)₅), 10.3 (s, C₅(CH₃)₅); $^{13}C\{^1H\}$ NMR ([D₈]THF, -80 °C): $\delta = 242.9$ (d, $J_{CP} = 11.5$ Hz, ReC), 182.8, 176.4(2), 175.4(2), 171.6, 170.7, 170.6, 166.2 (s, 9 CO), 154.0 (s, 1 C of ReCCCC),^[36] 136.1–129.0 (3 C₆H₅), 118.9, 115.5 (s, 2 C of ReCCCC),^[36] 101.4 (s, C₅(CH₃)₅), 10.2 (s, C₅(CH₃)₅); $^{31}P\{^1H\}$ NMR (CD_2Cl_2): $\delta = 21.4$ (s); MS (positive Cs-FAB, 2-nitrophenyl octyl ether/CH₂Cl₂):^[35] m/z : 1485 [7^+] (100 %), no other peaks > 10 % above $m/z > 300$.

[(η^5 -C₅Me₅)Re(NO)(PPh₃)(CC)Os₃(CO)₁₀(H)₂]⁺X⁻ (8⁺X⁻**):**

Method A: A Schlenk flask was charged with **2** (0.025 g, 0.016 mmol) and CH₂Cl₂ (10 mL) and cooled to -45 °C (NCCH₃/CO₂). The solution was stirred and HBF₄ · OEt₂ (2.5 μ L, 0.003 g, 0.016 mmol) was added. After 10 min, the cold bath was removed. After 1 h, the solution was filtered through Celite (1 cm plug). Solvent was removed from the filtrate under vacuum (oil-pump) to give **8⁺BF₄⁻** as an orange powder retaining approximately 0.5 equiv hexane (0.018 g, 0.011 mmol, 69 %),^[34e] m.p. 199–201 °C (decomp). C₄₀H₃₂BF₄NO₁₁Os₃PRE · (C₆H₁₄)_{0.5}: calcd C 31.87, H, 2.43; found C 31.38, H 2.49; IR (CH_2Cl_2): $\tilde{\nu} = 2137$ (m), 2110 (s), 2076 (s), 2058 (s), 2042 (s), 2006 (m), 1701 (w), 1674 cm⁻¹ (s); 1H NMR (CD_2Cl_2): $\delta = 7.97$ –7.90, 7.68–7.25 (m, 3 Ph), 1.78 (s, C₅Me₅), -15.68 (d, $J_{HH} = 0.9$ Hz, OsH), -19.39 (d, $J_{HH} = 0.9$ Hz, OsH);^[34e] $^{31}P\{^1H\}$ NMR (CD_2Cl_2): $\delta = 22.8$ (s).

Method B: A Schlenk flask was charged with **8⁺ · BF₄⁻** (0.025 g, 0.015 mmol), acetone (10 mL), and NaSbF₆ (0.044 g, 0.170 mmol). The sample was stirred for 1 h, and solvent was removed under vacuum (oil-pump). The residue was dissolved in CH₂Cl₂ (5 mL) and filtered through Celite (2 cm plug). Solvent was removed under vacuum (oil-pump) to give an orange oil. An acetone solution of the oil was layered with benzene (1:1 v/v). This gave orange prisms of **8⁺ · SbF₆⁻ · acetone · C₆H₆** that were used for crystallography. IR (CH_2Cl_2): $\tilde{\nu} = 2100$ (w), 2043 (s), 2031 (s), 2010 (vs), 1989 (m), 1979 (s), 1966 (m), 1940 (m), 1673 cm⁻¹ (m).

[(η^5 -C₅Me₅)Re(NO)(PPh₃)(CC)Os₃(CO)₉(OMe)] (10): A Schlenk flask was charged with **9**^[12] (0.025 g, 0.016 mmol) and heptane (10 mL) and fitted with a condenser. The solution was refluxed and stirred (4 h), and then cooled to room temperature. Solvent was removed under vacuum (oil-pump). Thin-layer chromatography of the residue (silica gel; hexane/CH₂Cl₂ 1:1 (v/v)) gave two orange bands (**9**, **10**). The second was extracted with CH₂Cl₂. The extract was concentrated (approx. 1 mL), and hexane was added (10 mL). Solvent was removed under vacuum (oil-pump) to give **10** as a red-orange powder retaining ≥ 0.5 equiv hexane (0.016 g, 0.011 mmol, 63 %). The sample was dissolved in CH₂Cl₂ and layered with hexane (sealed vial). This gave red prisms that were dried under an N₂ flow and used for crystallography (0.0095 g, 0.006 mmol),^[34f] m.p. 172–174 °C. C₄₁H₃₃NO₁₁Os₃PRE · (C₆H₁₄)_{0.5}: calcd C 34.17, H, 2.61; found (two samples) C 34.09/34.46, H 2.57/2.64; IR (CH_2Cl_2): $\tilde{\nu} = 2067$ (m), 2044 (s), 2015 (s), 1979 (s), 1961 (s), 1668 cm⁻¹ (w); 1H NMR (CD_2Cl_2): $\delta = 7.60$ –7.45 (m, 3 Ph), 3.79, 3.51 (2s, 48.0:52.0, OMe), 1.76, 1.73 (2s, 47.7:52.3, C₅Me₅);^[34f] $^{31}P\{^1H\}$ NMR (CD_2Cl_2): $\delta = 23.6$, 22.0, 21.6 (3s, 52.6:19.7:27.7); MS (positive Cs-FAB, 3-NBA/CH₂Cl₂):^[35] m/z : 1505 [M^+] (50 %; see Figure 5), 1478 [$M^+ - CO + 1$] (100 %), no other peaks > 30 % above 400.

Crystallography: Data were collected for **2** · (C₆H₁₄)_{0.5}, **8⁺ · SbF₆⁻ · acetone · C₆H₆**, and **10** · (C₆H₁₄)_{0.5} as outlined in Table 1. Cell constants were obtained from 25 reflections ($11^\circ < 2\theta < 28^\circ$; $2^\circ < 2\theta < 24^\circ$; $25^\circ < 2\theta < 30^\circ$). Space groups were determined from systematic absences ($h0l$ $h+l=2n$, $0k0$ $k=2n$; $h0l$ $h+l=2n$, $0k0$ $k=2n$; none) and subsequent least-squares refinement. Standard reflections (every 200 scans) showed no decay. Lorentz, polarization, and empirical absorption (Ψ scans) corrections were applied. The structures were solved by standard heavy-atom techniques with the MOLEN VAX package, and refined with SHELXL-93.^[37] Non-hydrogen atoms were refined anisotropically, except for the hexane solvate and disordered OMe atoms of **10** (which refined to a 62(4):38(4) O81/O81' occupancy). The osmium hydrides were located and refined isotropically. Other hydrogen atom positions were calculated and added to the structure factor calculations. Scattering factors, and $\Delta f'$ and $\Delta f''$ values, were taken from the literature.^[38] Crystallographic data (excluding structure factors) for **8⁺ · SbF₆⁻ · acetone · C₆H₆** and **10** · (C₆H₁₄)_{0.5}^[39] and an ORTEP with the minor form of the latter, have been deposited with the Cambridge Crystallographic Data Centre as Supplementary Publication no. CCDC-100854. Copies of the data can be obtained free of charge on application to CCDC, 12 Union Road, Cambridge CB21EZ, UK (Fax: (+44) 1223-336-033; e-mail: deposit@ccdc.cam.ac.uk).

Acknowledgment: We thank the DOE for support of this research, and Professor Richard Adams for valuable counsel.

Received: November 27, 1997 [F909]

[1] General reviews or perspectives: a) W. Beck, B. Niemer, M. Wieser, *Angew. Chem.* **1993**, *105*, 969; *Angew. Chem. Int. Ed. Engl.* **1993**, *32*,

- 923; b) H. Lang, *ibid.* **1994**, *106*, 569 and **1994**, *33*, 547; c) U. Bunz, *ibid.* **1996**, *108*, 1047 and **1996**, *35*, 969.
- [2] a) W. Weng, T. Bartik, M. Brady, B. Bartik, J. A. Ramsden, A. M. Arif, J. A. Gladysz, *J. Am. Chem. Soc.* **1995**, *117*, 11922; b) T. Bartik, B. Bartik, M. Brady, R. Dembinski, J. A. Gladysz, *Angew. Chem.* **1996**, *108*, 467; *Angew. Chem. Int. Ed. Engl.* **1996**, *35*, 414; c) B. Bartik, R. Dembinski, T. Bartik, A. M. Arif, J. A. Gladysz, *New J. Chem.* **1997**, *21*, 739; d) M. Brady, W. Weng, Y. Zhou, J. W. Seyler, A. J. Amoroso, A. M. Arif, M. Böhme, G. Frenking, J. A. Gladysz, *J. Am. Chem. Soc.* **1997**, *119*, 775.
- [3] a) N. Le Narvor, L. Toupet, C. Lapinte, *J. Am. Chem. Soc.* **1995**, *117*, 7129; b) F. Coat, C. Lapinte, *Organometallics* **1996**, *15*, 477; c) M. I. Bruce, L. I. Denisovich, P. J. Low, S. M. Peregudova, N. A. Ustynyuk, *Mendeleev Commun.* **1996**, 200; d) M. I. Bruce, M. Ke, P. J. Low, *Chem. Commun.* **1996**, 2405; e) B. E. Woodworth, P. S. White, J. L. Templeton, *J. Am. Chem. Soc.* **1997**, *119*, 828.
- [4] a) W. Weng, J. A. Ramsden, A. M. Arif, J. A. Gladysz, *J. Am. Chem. Soc.* **1993**, *115*, 3824; b) W. Weng, T. Bartik, J. A. Gladysz, *Angew. Chem.* **1994**, *106*, 2272; *Angew. Chem. Int. Ed. Engl.* **1994**, *33*, 2199.
- [5] a) M. D. Ward, *Chem. Ind.* **1996**, 568; b) M. D. Ward, *ibid.* **1997**, 640; c) D. Astruc, *Acc. Chem. Res.* **1997**, *30*, 383.
- [6] a) J. S. Bradley, *Adv. Organomet. Chem.* **1983**, *22*, 1; b) Review of C_2 complexes: M. Akita, Y. Moro-oka, *Bull. Chem. Soc. Jpn.* **1995**, *68*, 420; c) *The Chemistry of Transition Metal Carbides and Nitrides* (Ed.: S. T. Oyama), Blackie/Chapman and Hall, New York, **1996**.
- [7] For lead references, see: a) G. H. Worth, B. H. Robinson, J. Simpson, *Organometallics* **1992**, *11*, 3863; b) D. Osella, O. Gambino, C. Nevi, M. Ravera, D. Bertolino, *Inorg. Chim. Acta* **1993**, *206*, 155.
- [8] D. Miguel, M. Moreno, J. Pérez, V. Riera, D. G. Churchill, M. R. Churchill, T. S. Janik, *J. Am. Chem. Soc.* **1998**, *120*, 417.
- [9] Dicobalt clusters $Co_2(CO)_6$ have been joined by η^2, μ_2 linkages to a cyclic carbon chain. See: F. Diederich, Y. Rubin, O. L. Chapman, N. S. Goroff, *Helv. Chim. Acta* **1994**, *77*, 1441, and references therein.
- [10] a) C. J. Adams, M. I. Bruce, E. Horn, B. W. Skelton, E. R. T. Tiekink, A. H. White, *J. Chem. Soc. Dalton Trans.* **1993**, 3299 and 3313; b) D. M. Norton, C. L. Stern, D. F. Shriver, *Inorg. Chem.* **1994**, *33*, 2701.
- [11] S. B. Falloon, A. M. Arif, J. A. Gladysz, *Chem. Commun.* **1997**, 629.
- [12] S. B. Falloon, W. Weng, A. M. Arif, J. A. Gladysz, *Organometallics* **1997**, *16*, 2008.
- [13] J. A. Ramsden, W. Weng, J. A. Gladysz, *Organometallics* **1992**, *11*, 3635.
- [14] W. Weng, T. Bartik, M. T. Johnson, A. M. Arif, J. A. Gladysz, *Organometallics* **1995**, *14*, 889.
- [15] A. K. Smith, in *Comprehensive Organometallic Chemistry II, Vol. 7* (Eds.-in-Chief: E. W. Abel, F. G. A. Stone, G. Wilkinson; Volume Eds.: D. F. Shriver, M. I. Bruce), Pergamon, New York, **1995**, ch. 13.1–13.2.
- [16] J. Manna, K. D. John, M. D. Hopkins, *Adv. Organomet. Chem.* **1995**, *38*, 79.
- [17] A. J. Deeming, S. Hasso, M. Underhill, *J. Chem. Soc. Dalton Trans.* **1975**, 1614.
- [18] M. I. Bruce, B. W. Skelton, A. H. White, N. N. Zaitseva, *J. Chem. Soc. Dalton Trans.* **1996**, 3151. Related reactions are described in ref. [3d].
- [19] a) R. D. Adams, J. E. Babin, *Organometallics* **1988**, *7*, 2300; b) R. D. Adams, M. P. Pompeo, J. T. Tanner, *ibid.* **1991**, *10*, 1068.
- [20] In C_6D_5Cl , NMR spectra showed 92–89:8–11 mixtures of the two major isomers (1H , $\delta = 4.03, 3.55$ and $1.89, 1.80$; ^{31}P , 23.8, 25.0). In each of these cases, a small third peak (approx. 2%) was also present (ref. [21]).
- [21] These did not coalesce at 35 °C (CD_2Cl_2). When 1H NMR spectra were recorded at –80 or –100 °C, another set of pentamethylcyclopenta-dienyl signals appeared to be present (approx. 5%). We speculate that the PPH_3 signals at $\delta = 22.0$ and 21.6 represent propeller diastereomers: H. Brunner, R. Oeschey, B. Nuber, *Angew. Chem.* **1994**, *106*, 941; *Angew. Chem., Int. Ed. Engl.* **1994**, *33*, 866.
- [22] S. Aime, W. Dastrù, R. Gobetto, L. Milone, A. Viale, *Chem. Commun.* **1997**, 267.
- [23] There are many other related reactions that could be discussed (ref. [15]). For example, tungsten alkynyl complexes $[(\eta^5-C_5R_5)W(CO)_3(C\equiv CR')]$ and $[Os_3(CO)_{10}(NCMe)_2]$ react in refluxing toluene to give tetranuclear products of formula $[(\eta^5-C_5R_5)WO_3(CO)_{11}(C\equiv CR')]$. See: Y. Chi, C. Chung, Y.-C. Chou, P.-C. Su, S.-J. Chiang, S.-M. Peng, G.-H. Lee, *Organometallics* **1997**, *16*, 1702 and references therein.
- [24] Until 1996, we reported all E^\ominus values relative to a ferrocene E^\ominus value of 0.56 V. A recent review (N. G. Connelly, W. E. Geiger, *Chem. Rev.* **1996**, *96*, 877) has proposed protocols for standardizing E^\ominus values from a variety of solvent/electrolyte combinations to a common SCE reference. These employ ferrocene E^\ominus values of 0.46 V in $CH_2Cl_2/n-Bu_4N^+PF_6^-$. In order to facilitate comparisons of our data and literature E^\ominus values, we will adopt this convention henceforth.
- [25] Review: D. Röttger, G. Erker, *Angew. Chem.* **1997**, *109*, 840; *Angew. Chem. Int. Ed. Engl.* **1997**, *36*, 813.
- [26] Additional references: a) K. Sorger, P. v. R. Schleyer, R. Fleischer, D. Stalke, *J. Am. Chem. Soc.* **1996**, *118*, 6924; b) C. J. Adams, M. I. Bruce, B. W. Skelton, A. H. White, *Chem. Commun.* **1996**, 975; c) G. Frapper, J.-F. Halet, M. I. Bruce, *Organometallics* **1997**, *16*, 2590.
- [27] K. B. Wiberg, *Acc. Chem. Res.* **1984**, *17*, 379.
- [28] a) M. D. Jones, R. D. W. Kemmitt, *Adv. Organomet. Chem.* **1987**, *27*, 279; b) G. Rodriguez, G. C. Bazan, *J. Am. Chem. Soc.* **1997**, *119*, 343.
- [29] P. L. Bogdan, C. Woodcock, D. F. Shriver, *Organometallics* **1987**, *6*, 1377 and references therein.
- [30] R. P. Andres, J. D. Bielefeld, J. I. Henderson, D. B. Janes, V. R. Kolagunta, C. P. Kubiak, W. J. Mahoney, R. G. Osifchin, *Science* **1996**, *273*, 1690.
- [31] M. Altmann, J. Friedrich, F. Beer, R. Reuter, V. Enkelmann, U. H. F. Bunz, *J. Am. Chem. Soc.* **1997**, *119*, 1472.
- [32] J. A. Ramsden, W. Weng, J. A. Gladysz, *Organometallics* **1992**, *11*, 3635.
- [33] S. Aime, A. J. Deeming, *J. Chem. Soc. Dalton Trans.* **1983**, 1809.
- [34] Hexane 1H NMR (CD_2Cl_2): $\delta = 1.26$ – 1.27 (m; 4 CH_2), 0.87–0.88 (t; 2 CH_3). Stoichiometry based upon integration: a) 0.44 equiv (powder) to 0.46 equiv (crystals); b) 0.25 equiv; c) 0.56 equiv; d) 0.37 equiv; e) 0.57 equiv; f) 0.48 equiv (crystals). All mmol and yield calculations correct for the solvate.
- [35] Each m/z value is for the most intense peak of the isotope envelope; relative intensities are for the specified mass range.
- [36] These assignments are provisional.
- [37] a) B. A. Frenz, in *The Enraf–Nonius CAD 4 SDP – A Real-time System for Concurrent X-Ray Data Collection and Crystal Structure Determination in Computing and Crystallography* (Eds.: H. Schenk, R. Olthof-Hazelkamp, H. van Koningsveld, G. C. Bassi), Delft University Press, Delft (The Netherlands) **1978**, pp. 64–71; b) G. M. Sheldrick, *SHELXS-93 Program for Crystal Structure Refinement*, Universität Göttingen, **1993**.
- [38] D. T. Cromer, J. T. Waber in *International Tables for X-Ray Crystallography, Vol. IV* (Eds.: J. A. Ibers, W. C. Hamilton), Kynoch, Birmingham (UK) **1974**.
- [39] Data for $2 \cdot (\text{hexane})_{0.5}$ were deposited in the Cambridge Crystallographic Database upon publication of our preliminary communication (ref. [11]).